PERGAMON

International Journal of Solids and Structures 40 (2003) 6429–6444

INTERNATIONAL JOURNAL OF SOLIDS and STRUCTURES

www.elsevier.com/locate/ijsolstr

Passing stiffness anisotropy in multilayers and its effects on nanoscale surface self-organization

Y.F. Gao *

Department of Mechanical and Aerospace Engineering, Princeton University, Princeton, NJ 08544, USA

Received 9 December 2002

Abstract

A binary monolayer adsorbed on a solid surface can separate into distinct phases that further self-assemble into various two-dimensional patterns. The surface stresses in the two phases are different, causing an elastic field in the substrate. The self-organization minimizes the combined free energy of mixing, phase boundary, and elasticity. One can obtain diverse patterns by using substrates with various crystalline symmetries. Consider the pattern of a set of periodic stripes. The stripe orientation depends on the anisotropy in surface stress, substrate stiffness, and phase boundary energy. A more powerful and flexible way is to use a layered substrate. Surface properties designed for the applications of those patterns can be obtained by choosing appropriate materials and structures for the monolayer and the top layer of the substrate. The subsequent layers of the substrate provide the required stiffness anisotropy, the effect of which is passed to the monolayer patterns through the elastic field. We solve the elastic field in the anisotropic, heterogeneous, three-dimensional half-space by using the Eshelby–Stroh–Lekhnitskii formalism and the Fourier transformation. Depending on the thicknesses and the degrees of the stiffness anisotropy of the substrate layers, the lowest energy stripes can have tunable equilibrium size and orientation. We also discuss other possibilities of manipulating the phase patterns by engineering the elastic field.

Keywords: Nanostructure; Self-organization; Surface stress; Multilayer; Anisotropic elasticity

1. Introduction

One challenge in nanofabrication is to make large-scale ordered and patterned structures with nanoscale features, which would open new possibilities for applications, e.g., serving as memories, or as templates for making devices. Mesoscopic self-organization on solid surfaces offers many opportunities in making such nanostructures. Experiments have shown that adsorbed monolayers on solid surfaces, when separating into

* Present address: Division of Engineering, Box D, Brown University, Providence, RI 02912, USA. Tel.: +1-401-863-2872; fax: +1-401-863-9009.

E-mail address: yanfei_gao@brown.edu (Y.F. Gao).

0020-7683/$ - see front matter © 2003 Elsevier Ltd. All rights reserved.
doi:10.1016/S0020-7683(03)00373-1

distinct phases, can self-assemble into various two-dimensional patterns (Kern et al., 1991; Zeppenfeld et al., 1995; Pohl et al., 1999; Ellmer et al., 2001). The observed feature sizes of the phase patterns range from nanometers to hundreds of micrometers, and are usually stable on annealing. The limited tunability of the phase patterns impedes the use of these nanostructures. In the following, we first briefly review the mechanism of pattern formation, and then examine how to guide these self-assembled phase patterns into designed order.

The self-organization minimizes the combined free energy of mixing, phase boundary, and an elastic field (Alerhand et al., 1988; Ng and Vanderbilt, 1995; Suo and Lu, 2000). Suppose that the monolayer consists of two atomic species, one of which could be identical to that of the substrate. When the two species have a large enthalpy of mixing, atoms are more likely to be found near identical atoms than if they were mixed randomly. Consequently, the monolayer separates into two phases, and the concentration field on the solid surface becomes nonuniform. The surface stresses in the two phases are different (Ibach, 1997), inducing an elastic field in the substrate. To relieve the surface stress nonuniformity, large phases will break into small phases. The total length of phase boundaries, however, increases and so does the phase boundary energy. It is the competition between the phase boundary energy and the elastic energy that stabilizes the phase patterns and selects an equilibrium phase size.

Because the surface stress difference in distinct phases is accommodated through the substrate deformation, one immediate way to manipulate the phase patterns is to modify the elastic field. Previously, we have studied the effect of symmetry breaking of various modes on phase patterns. When the system was isotropic, there was no preferred orientation in the plane of the monolayer, and therefore irregular patterns formed. When some form of anisotropy was introduced, the symmetry was broken, and irregular patterns lined up in some particular directions. We investigated how to obtain diverse patterns by using substrates with various crystalline symmetries (Lu and Suo, 2002b; Gao and Suo, 2003b). Stripes could orient along either the crystalline axes, or certain directions off them. The off-axis stripes might organize into a mesoscale herringbone structure, further relaxing the elastic energy (Lu and Suo, 2002a; Gao et al., 2002). Phase diagrams were constructed with respect to varying parameters that represented anisotropy in phase boundary energy, surface stress, and substrate stiffness.

This paper investigates the possibility of manipulating the self-assembled monolayer patterns by using a layered substrate. Surface stress and phase boundary energy, depending on the short-range interatomic interactions, can vary considerably with different material and structural selections of the monolayer and the first substrate layer. The subsequent underlying layers of the substrate provide certain degrees of stiffness anisotropy, the effect of which is passed to the monolayer patterns through the long-range elastic field. Those considerations give rise to a large parameter space that can be used to tailor the experiments.

As illustrated in Section 2, the elastic field in the substrate is coupled with the concentration field on the substrate surface through the concentration-dependent surface stress. We use the Fourier series to represent the concentration field of a set of periodic stripes. The equilibrium stripe orientation can be determined by minimizing a free energy function, as shown in Section 3. This study is concentrated on how to manipulate the phase patterns by engineering the elastic field, so that the phase boundary energy is assumed isotropic throughout this paper. The elasticity boundary value problem is solved by using the Eshelby–Stroh–Lekhnitskii representation (Eshelby et al., 1953; Stroh, 1958; Lekhnitskii, 1963; Suo, 1990; Ting, 1996; Gao and Suo, 2003b). Section 4 assumes that the substrate is a homogeneous material, and studies the orientation of stripes on the (1 0 0) surface of a cubic crystal with anisotropic surface stress. Section 5 gives the general elastic solution in a layered structure, and studies the stripes on the substrate of two different isotropic materials, an isotropic material on a cubic crystal, and two cubic crystals. Any crystal plane and elastic anisotropy can be treated, and the equilibrium size and orientation are tunable. Section 6 discusses other possibilities to affect the elastic field and manipulate the phase patterns.

2. Substrate deformation caused by monolayer concentration nonuniformity

Fig. 1 shows the system to be modeled. The monolayer coincides with the plane (x_1, x_2). Let a continuous function $C(x_1, x_2)$ be the concentration field in the monolayer. The substrate is semi-infinite, occupying the half space $x_3 < 0$. The substrate may be a homogeneous material or a layered structure. The layers are different in constituting materials or crystalline orientations. We assume that the layer interfaces parallel with each other, so that the substrate is heterogeneous only in the x_3 direction.

The surface stress is the excess work per unit area done when the surface enlarges per unit strain (Ibach, 1997). In general, the surface stress is a second-rank tensor $f_{\alpha\beta}$. (Greek subscripts run from 1 to 2.) We assume that the surface stress is linear in the concentration C. That is, when the concentration changes by ΔC, the surface stress changes by

$$\Delta f_{\alpha\beta} = \phi_{\alpha\beta} \Delta C. \tag{1}$$

The slope tensor $\phi_{\alpha\beta}$ depends on the materials system of the adlayer and several marginal atomic layers of the substrate. It can be measured by the wafer curvature method, or determined by electronic structure calculations. We treat it phenomenologically in this study.

As illustrated in Fig. 1, the principal components of the slope tensor, ϕ_1 and ϕ_2, are assumed to be in the direction x_1 and x_2. Following Gao and Suo (2003b), we define the surface stress anisotropy parameter as

$$R = \frac{\phi_2 - \phi_1}{\sqrt{2}\phi}, \tag{2}$$

where $\phi = \sqrt{\phi_1^2 + \phi_2^2}$ measures the magnitude of the slope tensor. R is in the range $-1 \leqslant R < 1$. When $R = 0$, $\phi_1 = \phi_2$, and the slope tensor is isotropic. We should point out that even if the substrate is elastically isotropic, the surface stress could be anisotropic because of the possibly anisotropic atomic structure in the adlayer (Ng and Vanderbilt, 1995; Ibach, 1997).

When the concentration field is uniform, from (1), the surface stress is also uniform, so that the semi-infinite substrate is unstrained. When the concentration field is nonuniform, corresponding to concentration patterns, the surface stress is also nonuniform, causing an elastic field in the substrate. The elasticity boundary value problem is specified as follows.

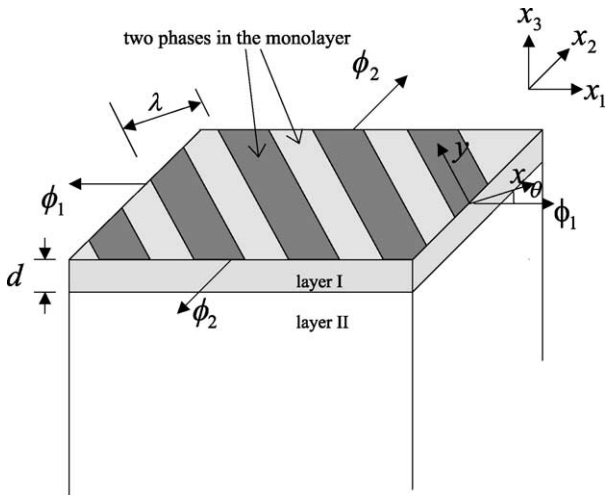

Fig. 1. Schematic representation of the monolayer–substrate system. The substrate can be a layered structure.

Assume that the deformation in the substrate is infinitesimal, and each layer of the substrate is linearly elastic and generally anisotropic. The stress tensor σ_{ij} relates to the elastic displacement vector u_i as

$$\sigma_{ij} = c_{ijkl} u_{k,l}, \tag{3}$$

where, l stands for differentiation with respect to the coordinate x_l. Latin subscripts run from 1 to 3. The repeated subscripts imply the summation convention. For each layer, the stiffness tensor c_{ijkl} is known once the material and its crystallographic orientation are specified.

The equations of mechanical equilibrium are standard, i.e., $\sigma_{ij,j} = 0$. Together with (3), we can write the field equations that govern the elastic displacements:

$$c_{ijkl} u_{k,lj} = 0. \tag{4}$$

We will have N sets of such equations if there are N layers. The traction vector $\mathbf{t} = (\sigma_{31}, \sigma_{32}, \sigma_{33})^{\mathrm{T}}$ on the substrate surface ($x_3 = 0$) is (Suo and Lu, 2000; Gao and Suo, 2003b)

$$\mathbf{t} = \left(\phi_1 \frac{\partial C}{\partial x_1}, \phi_2 \frac{\partial C}{\partial x_2}, 0 \right)^{\mathrm{T}}. \tag{5}$$

The normal traction σ_{33} is zero because there is no z-component of the surface stress tensor. There could be other mechanisms leading to the normal component (Gurtin and Murdoch, 1976; Murdoch, 1976; Thomson et al., 1986). However, our above argument is generally true for adsorbate-induced surface stresses (Ibach, 1997). This fact tells us that any normal deformation will not affect the elastic free energy, as will be shown in Eq. (6) shortly. Assume that the layers are ideally bonded at the interfaces, and we will have $2(N-1)$ continuity conditions. Another boundary condition is that the stress tensor vanishes as $x_3 \to -\infty$.

Consequently, for any given concentration field $C(x_1, x_2)$, the elastic equilibrium defines an elasticity boundary value problem in the semi-infinite, anisotropic, heterogeneous substrate with prescribed surface traction. We combine the Eshelby–Stroh–Lekhnitskii formalism (Eshelby et al., 1953; Stroh, 1958; Lekhnitskii, 1963; Suo, 1990; Ting, 1996) and the Fourier transformation to determine the elastic field.

One can easily confirm that the elastic energy stored in the volume of the substrate is $\int (1/2)\sigma_{3\alpha} u_\alpha \, \mathrm{d}A$, a positive quantity. The integral extends over the entire substrate surface. Since the traction boundary condition is fixed, in building up the elastic field in the substrate, the traction does work $\int \sigma_{3\alpha} u_\alpha \, \mathrm{d}A$. This work comes from the surface stress difference between distinct phases, and reduces the total free energy of the monolayer–substrate system. Consequently, the elastic free energy is

$$G_{\mathrm{elastic}} = \int \frac{1}{2} \sigma_{3\alpha} u_\alpha \, \mathrm{d}A - \int \sigma_{3\alpha} u_\alpha \, \mathrm{d}A = - \int \frac{1}{2} \sigma_{3\alpha} u_\alpha \, \mathrm{d}A, \tag{6}$$

which can also be confirmed from the Legendre transformation. The elastic free energy is always negative. The larger the elastic deformation in the substrate, the lower the free energy of the monolayer–substrate system.

With a given traction boundary condition (5), the strain and the displacement fields are linear in the compliance tensor. Consequently, the elastic free energy is also linear in the compliance tensor, and is quadratic in the slope tensor $\phi_{\alpha\beta}$. The last observation shows that the sign of the slope tensor does not matter.

The total free energy of the monolayer–substrate system can be written as

$$G = \int \left(g_{\mathrm{m}} + g_{\mathrm{b}} - \frac{1}{2} \sigma_{3\alpha} u_\alpha \right) \mathrm{d}A. \tag{7}$$

The term g_m represents the free energy of mixing, and is a function of the concentration. The phase boundary energy, represented by the term g_b, in general is a function of the concentration and the concentration gradient. Detailed forms of g_m and g_b are unimportant to this work.

3. Equilibrium orientation of periodic stripes

Consider a set of periodic stripes as shown in Fig. 1. The concentration is now nonuniform, and constrained to vary in the direction x. The orientation angle θ is measured from the x_1 axis to the x axis. Represent the concentration field by a Fourier series,

$$C(x) = \sum_{n=-\infty}^{+\infty} C_n \exp\left(\frac{\mathrm{i}2n\pi x}{\lambda}\right) = \sum_{n=-\infty}^{+\infty} C_n \exp\left[\frac{\mathrm{i}2n\pi}{\lambda}(h_1 x_1 + h_2 x_2)\right], \tag{8}$$

where $x = h_\alpha x_\alpha$, $(h_1, h_2) = (\cos\theta, \sin\theta)$ is the direction vector of axis x in coordinates (x_1, x_2), and λ is the period of the concentration field. To ensure the concentration is real-valued, we require that $C_{(-n)} = \overline{C}_n$, where a bar on the top of a quantity denotes the complex conjugate. The average concentration C_0 remains constant, since no atoms leave or enter the monolayer during annealing.

From (5) and (8), the traction vector on the substrate surface ($x_3 = 0$) becomes

$$\begin{aligned}
\sigma_{31} &= \mathrm{i}\phi_1 h_1 \sum_{n=-\infty}^{+\infty} \frac{2n\pi C_n}{\lambda} \exp\left[\frac{\mathrm{i}2n\pi}{\lambda}(h_1 x_1 + h_2 x_2)\right], \\
\sigma_{32} &= \mathrm{i}\phi_2 h_2 \sum_{n=-\infty}^{+\infty} \frac{2n\pi C_n}{\lambda} \exp\left[\frac{\mathrm{i}2n\pi}{\lambda}(h_1 x_1 + h_2 x_2)\right], \\
\sigma_{33} &= 0.
\end{aligned} \tag{9}$$

As will become clear later, such a Fourier representation will simplify the solution of the elasticity boundary value problem.

The free energy density of mixing, g_m, is independent of θ. We assume that the phase boundary energy is isotropic in this study, so that g_b is also independent of θ. So long as the θ-dependence is concerned, G_{elastic} represents the free energy.

The elastic free energy per unit area is calculated by the elastic free energy in a period divided by the period, namely,

$$\widetilde{G}_{\text{elastic}} = -\frac{1}{\lambda}\int_0^{\lambda} \frac{1}{2}\sigma_{3\alpha}u_\alpha \,\mathrm{d}x. \tag{10}$$

Consequently, the equilibrium orientation of a set of periodic stripes can be determined by minimizing Eq. (10) as a function of θ with varying period λ, Fourier coefficients C_n ($n \neq 0$), and parameters that represent anisotropy.

4. Stripes on a homogeneous substrate

Consider a substrate of a single material with a given crystalline orientation. This substrate is subject to surface tractions (9), and therefore the elastic field is a plane field in the plane spanned by x_3 and the vector (h_1, h_2). From (9), since generally $\phi_2 \neq 0$, the substrate deformation is a combination of the inplane and antiplane strain field. We solve this plane field by using the Eshelby–Stroh–Lekhnitskii formalism. The

solution method discussed below basically follows Gao and Suo (2003b), and will be extended to a layered structure in Section 5.

Since the field equations (4) are homogeneous, we look for solution of the form

$$u_l = A_l f(z), \quad z = x + px_3 = h_1 x_1 + h_2 x_2 + px_3. \tag{11}$$

Here f is a one-variable function, p a scalar, and A_l a vector. As will be clear shortly, p is a complex number. Substitute (11) into (4), write $p = h_3$, and we obtain that

$$c_{ijlm} h_j h_m A_l = 0. \tag{12}$$

In deriving (12), we have eliminated the factor $\mathrm{d}^2 f/\mathrm{d}z^2$. To obtain a nontrivial solution of vector A_l, the coefficient matrix $c_{ijlm} h_j h_m$ must be singular, i.e., $\det(c_{ijlm} h_m h_j) = 0$. This is a generalized eigenvalue problem with p being the eigenvalue and A_l the eigenvector.

Remember h_1 and h_2 are direction cosines of axis x, and $h_3 = p$, so that $\det(c_{ijlm} h_m h_j)$ is a sixth-order polynomial in p with real coefficients. If p were also real, the matrix $c_{ijlm} h_m h_j$ would be positive-definite (due to the requirement that the strain energy be positive), and the linear equations (12) would have only trivial solution. Therefore, the six roots form three pairs of complex conjugate. Denote the three eigenvalues with positive imaginary parts by p_a, $a = 1, 2, 3$, and the corresponding eigenvectors by A_{ka}. Once the stiffness tensor c_{ijkl} is specified, for a given direction (h_1, h_2), one can solve this eigenvalue problem (12) numerically.

Let $f_1(z_1)$, $f_2(z_2)$, $f_3(z_3)$ be three arbitrary analytic functions with respect to the three complex variables, $z_a = h_1 x_1 + h_2 x_2 + p_a x_3$, $a = 1, 2, 3$, respectively. The general solution of the displacement field is a linear superposition:

$$u_l = \sum_a A_{la} f_a(z_a) + \sum_a \overline{A}_{la} \bar{f}_a(\bar{z}_a). \tag{13}$$

This form ensures that the displacement is real-valued. The traction vector on any plane normal to the x_3 axis, $\mathbf{t} = (\sigma_{13}, \sigma_{23}, \sigma_{33})^{\mathrm{T}}$, is

$$\sigma_{i3} = \sum_a L_{ia} f_a'(z_a) + \sum_a \overline{L}_{ia} \bar{f}_a'(\bar{z}_a), \tag{14}$$

where the three vectors L_{ia} are defined as

$$L_{ia} = (c_{i3l1} h_1 + c_{i3l2} h_2 + c_{i3l3} p_{\underline{a}}) A_{l\underline{a}}. \tag{15}$$

No summation convention is implied over underscored, repeated subscripts.

The Stroh matrix $\mathbf{B} = \mathrm{i}\mathbf{A}\mathbf{L}^{-1}$ has been proven to be a positive-definite Hermitian (Stroh, 1958). Split the matrix into the real and the imaginary parts, $\mathbf{B} = \mathbf{M} + \mathrm{i}\mathbf{N}$, so that $\mathbf{M}$ is symmetric and positive-definite, and $\mathbf{N}$ is antisymmetric. These matrices have the same dimension as the compliance tensor. Though explicit expressions can be derived, for convenience, these matrices are calculated numerically.

To determine the three functions $f_1(z_1)$, $f_2(z_2)$, $f_3(z_3)$, we adopt the analytic continuation method developed by Suo (1990). Let ζ be a complex variable of the form $\zeta = h_1 x_1 + h_2 x_2 + q x_3$, where q is an arbitrary complex number with a positive imaginary part. Use the vector notation, $\mathbf{f}(\zeta) = [f_1(\zeta), f_2(\zeta), f_3(\zeta)]^{\mathrm{T}}$. On the plane $x_3 = 0$, the four complex variables, z_1, z_2, z_3, ζ, all equal $h_1 x_1 + h_2 x_2$, so that the traction vector and the displacement vector are

$$\mathbf{u} = \mathbf{A}\mathbf{f}(h_\alpha x_\alpha) + \overline{\mathbf{A}}\bar{\mathbf{f}}(h_\alpha x_\alpha), \tag{16}$$

$$\mathbf{t} = \mathbf{L}\mathbf{f}'(h_\alpha x_\alpha) + \overline{\mathbf{L}}\bar{\mathbf{f}}'(h_\alpha x_\alpha). \tag{17}$$

The traction on the substrate surface has been prescribed by a Fourier series in Eq. (9). By the principle of linear superposition, we consider only one real-valued component. That is, for a given pair of $\pm n$, the traction vector is

$$\mathbf{t} = \mathbf{a}\exp(\mathrm{i}\kappa_1 x_1 + \mathrm{i}\kappa_2 x_2) + \bar{\mathbf{a}}\exp(-\mathrm{i}\kappa_1 x_1 - \mathrm{i}\kappa_2 x_2), \tag{18}$$

where $\mathrm{i} = \sqrt{-1}$, $\kappa_\alpha = \kappa h_\alpha$, $\kappa = 2n\pi/\lambda$, and

$$\mathbf{a} = (\mathrm{i}\phi_1 h_1 \kappa C_n, \mathrm{i}\phi_2 h_2 \kappa C_n, 0)^{\mathrm{T}}. \tag{19}$$

The analytic functions $\mathbf{f}(\zeta)$ must both satisfy the traction boundary conditions (17) and (18), and vanish in the substrate far below the surface, namely, $\mathbf{f}(\zeta) \to 0$ as $x_3 \to -\infty$. The latter comes from the analytic continuation and the observation that the stress tensor, as well as $f_1(z_1)$, $f_2(z_2)$, $f_3(z_3)$, is vanishing with increasing depth. An inspection gives the solution

$$\mathbf{L}\mathbf{f}'(\zeta) = \bar{\mathbf{a}}\exp(-\mathrm{i}\kappa\zeta). \tag{20}$$

The fact that q in $\zeta = h_1 x_1 + h_2 x_2 + q x_3$ has positive imaginary part ensures that $\mathbf{f}(\zeta) \to 0$ as $x_3 \to -\infty$. From (16) and (20), the displacement on the substrate surface is

$$\mathbf{u} = \frac{\overline{\mathbf{B}}\mathbf{a}}{\kappa}\exp(\mathrm{i}\kappa_1 x_1 + \mathrm{i}\kappa_2 x_2) + \frac{\mathbf{B}\bar{\mathbf{a}}}{\kappa}\exp(-\mathrm{i}\kappa_1 x_1 - \mathrm{i}\kappa_2 x_2). \tag{21}$$

From (18) and (21), for one real-valued Fourier component of the traction boundary condition (9), the elastic energy stored in the substrate per period is given by

$$\frac{\kappa_1\kappa_2}{(2\pi)^2}\int_{-\pi/\kappa_2}^{\pi/\kappa_2}\int_{-\pi/\kappa_1}^{\pi/\kappa_1}\frac{1}{2}\mathbf{t}^{\mathrm{T}}\cdot\mathbf{u}\,\mathrm{d}x_1\,\mathrm{d}x_2 = \frac{\mathbf{a}^{\mathrm{T}}\mathbf{M}\bar{\mathbf{a}}}{\kappa}. \tag{22}$$

Consequently, the elastic free energy per unit area, with respect to arbitrary concentration field on the substrate surface, can be written as

$$\widetilde{G}_{\mathrm{elastic}} = -\phi^2\Theta\left(\frac{2\pi}{\lambda}\right)\sum_{n=1}^{+\infty}\left(nC_n^2\right), \tag{23}$$

where

$$\Theta = \mathbf{m}^{\mathrm{T}}\mathbf{M}\mathbf{m}, \tag{24}$$

$$\mathbf{m} = (h_1\cos\omega,\ h_2\sin\omega,\ 0)^{\mathrm{T}}. \tag{25}$$

In Eq. (23), Θ is the only term that depends on θ. Consequently, $-\Theta$ represents the free energy so long as the θ-dependence is concerned. Since the matrix $\mathbf{M}$ only depends on the stiffness tensor of the substrate, dimensionless vector $\mathbf{m}$ on direction θ and the surface stress anisotropy, the equilibrium stripe orientation θ_{eq}, at which $-\Theta$ minimizes, is independent of the concentration field.

On an elastically isotropic substrate, depending on the degree of the surface stress anisotropy (measured by the parameter R), the lowest energy stripes can be either parallel to, or at an angle from, the principal axis of the surface stress tensor. This phenomenon has been studied, and a physical interpretation has been given (Lu and Suo, 2002a; Gao et al., 2002). We next discuss the orientation of stripes on the (1 0 0) surface of a cubic crystal with anisotropic surface stress.

4.1. The (1 0 0) surface of a cubic crystal with anisotropic surface stress

The stiffness tensor of a cubic crystal has three independent components, i.e., c_{11}, c_{12}, c_{44} in the abbreviated notation. Define two dimensionless parameters:

$$\eta = c_{12}/c_{11}, \tag{26}$$

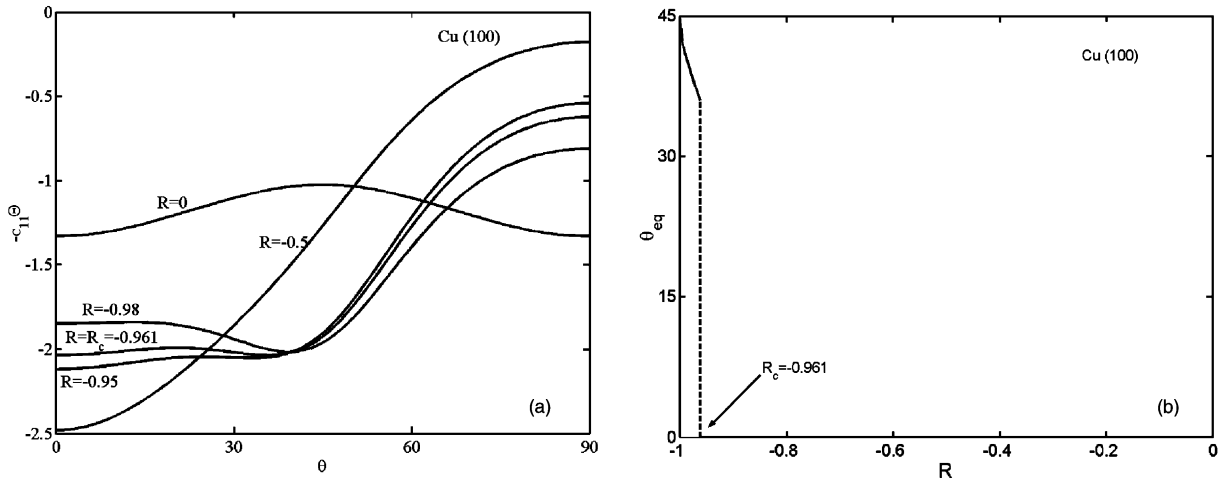

Fig. 2. (a) $-c_{11}\Theta$ as a function of θ for stripes on the Cu(1 0 0) surface. (b) The equilibrium orientation θ_{eq} as a function of R.

$$\xi = \frac{c_{12} + 2c_{44}}{c_{11}} - 1. \tag{27}$$

The requirement that the strain energy be positive for any arbitrary strain tensor places the following restrictions: $-0.5 < \eta < 1$, and $\eta - 1 < \xi < +\infty$. The parameter ξ measures the stiffness anisotropy of a cubic crystal. For an elastically isotropic material, $\xi = 0$, and $\eta = v/(1 - v)$, where v is Poisson's ratio. For Cu, $\eta = 0.721$, and $\xi = 0.6164$; for Mo, $\eta = 0.3826$, and $\xi = -0.1391$.

Fig. 2(a) plots $-c_{11}\Theta$ as a function of θ for the Cu(1 0 0) surface, and Fig. 3(a) for the Mo(1 0 0) surface. Symmetry operations dictate that once θ_{eq} is an equilibrium orientation, $-\theta_{eq}$ and $90° - \theta_{eq}$ are also. The multiplicity can be removed by restricting $0° \leqslant \theta_{eq} \leqslant 45°$ and $-1 \leqslant R \leqslant 0$. Depending on R, there are different kinds of behaviors. When $R = 0$, $\phi_1 = \phi_2$, the surface stress is isotropic. The strain and displacement fields are linear in the compliance tensor. Everything else being equal, because of the stiffness anisotropy, stripes in different orientations can induce different amount of elastic energy in the substrate. The shear

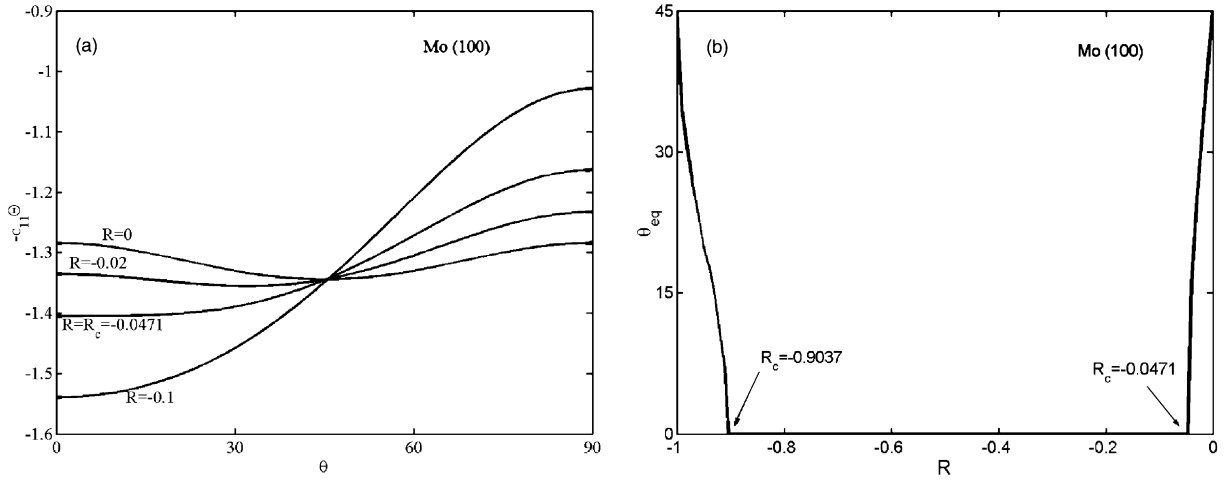

Fig. 3. (a) $-c_{11}\Theta$ as a function of θ for stripes on the Mo(1 0 0) surface. (b) The equilibrium orientation θ_{eq} as a function of R.

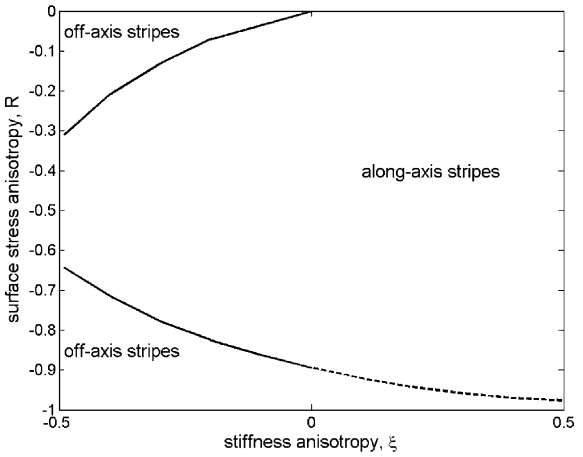

Fig. 4. Phase diagram of stripe orientation with varying R and ξ for the (1 0 0) surface of a cubic crystal ($\eta = 0.5$).

modulus in any (x, x_3) plane is the same, but the tensile modulus in x direction is not. Consequently, stripes with concentration field varying along the most compliant direction in tension will relax elastic energy the most. The tensile modulus in x direction reaches the minimum at $\theta_{eq} = 0°$ when $\xi > 0$, or $\theta_{eq} = 45°$ when $\xi < 0$ (Lu and Suo, 2002b), corresponding to the curves in Figs. 2(a) and 3(a) when $R = 0$.

We then examine the combined effect of stiffness anisotropy and surface stress anisotropy. Fig. 2(b) plots the equilibrium orientation θ_{eq} as a function of the surface stress anisotropy parameter R for stripes on the Cu(1 0 0) surface, and Fig. 3(b) for stripes on the Mo(1 0 0) surface. As shown in Fig. 2(a), for stripes on the Cu(1 0 0) surface, when $-0.961 < R < 0$, the equilibrium orientation is $\theta_{eq} = 0°$, and the equilibrium stripes are along the ϕ_2 axis. When R is slightly larger than $R_c = -0.961$, a new minimum appears at a nontrivial angle. When $R < R_c$, this minimum becomes lower than that at $\theta = 0°$. Consequently, the transition between the along-axis to off-axis stripes on the Cu(1 0 0) surface obeys the Landau theory of phase transition of the first-order, as indicated by the dashed line in Fig. 2(b). For stripes on the Mo(1 0 0) surface, when $-0.0471 < R \leqslant 0$ or $-1 \leqslant R < -0.9037$, the equilibrium stripes are off-axis. Between the two regions of off-axis stripes is the one of along-ϕ_2 stripes. As shown by Fig. 3(a), when $-0.0471 < R \leqslant 0$, the function $-c_{11}\Theta$ minimizes at a nontrivial angle. As R goes to $R_c = -0.0471$, θ_{eq} goes to 0°. Consequently, the transition between along-axis to off-axis stripes on the Mo(1 0 0) surface obeys the Landau theory of phase transition of the second-order.

Fig. 4 shows a phase diagram of the orientation of stripes on the (1 0 0) surface of a cubic crystal, with $\eta = 0.5$, and varying R and ξ. When $\xi > 0$, similar to the Cu(1 0 0) surface, we see the transition from the along-axis stripes to the off-axis ones. When $\xi < 0$, similar to the Mo(1 0 0) surface, we see the transition from the off-axis stripes, to the along-axis stripes, and back to the off-axis stripes.

The orientation of stripes on the (1 1 0) surface of a cubic crystal with anisotropic surface stress has been studied in Gao and Suo (2003b). Results presented there and in this paper suggest that one should observe various stripe orientations in different monolayer–substrate systems.

5. Stripes on a layered substrate

The geometrical conventions used in this section have been shown in Fig. 1. Consider a substrate of two layers. Layer I occupies the space $-d < x_3 < 0$, and layer II extends to $-\infty$. In each layer, the general solution of the elastic field in the plane spanned by vector (h_1, h_2) and axis x_3 has been given in Eqs. (13) and

(14). The remaining task is to determine the three functions $f_1(z_1)$, $f_2(z_2)$, $f_3(z_3)$ for each layer by the boundary and continuity conditions. The solution method developed in this section is quite general, and is likely to find applications in other phenomena, such as thin films, ferroelastic multilayers.

Different from (20), let the solution in the first substrate layer be

$$\mathbf{L}_{\mathrm{I}}\mathbf{f}'_{\mathrm{I}}(\zeta) = \mathbf{P}\exp(-\mathrm{i}\kappa\zeta) + \mathbf{Q}\exp(\mathrm{i}\kappa\zeta), \tag{28}$$

$$\mathbf{A}_{\mathrm{I}}\mathbf{f}_{\mathrm{I}}(\zeta) = \frac{\mathbf{B}_{\mathrm{I}}\mathbf{P}}{\kappa}\exp(-\mathrm{i}\kappa\zeta) - \frac{\mathbf{B}_{\mathrm{I}}\mathbf{Q}}{\kappa}\exp(\mathrm{i}\kappa\zeta), \tag{29}$$

where $\mathbf{P}$ and $\mathbf{Q}$ are two constant vectors to be determined.

From (28) and (29), one can readily obtain $f'_{\mathrm{I}1}(\zeta)$, $f'_{\mathrm{I}2}(\zeta)$, $f'_{\mathrm{I}3}(\zeta)$, and $f_{\mathrm{I}1}(\zeta)$, $f_{\mathrm{I}2}(\zeta)$, $f_{\mathrm{I}3}(\zeta)$. One then replaces the variable to $f'_{\mathrm{I}1}(z_1)$, $f'_{\mathrm{I}2}(z_2)$, $f'_{\mathrm{I}3}(z_3)$, and $f_{\mathrm{I}1}(z_1)$, $f_{\mathrm{I}2}(z_2)$, $f_{\mathrm{I}3}(z_3)$, and calculates the displacement field from (13) and the stress field from (14). The calculation gives the displacement and stress fields in the layer I:

$$\mathbf{u}_{\mathrm{I}} = \frac{\overline{\mathbf{E}}_{\mathrm{I}}^{-}\overline{\mathbf{P}} - \mathbf{E}_{\mathrm{I}}^{+}\mathbf{Q}}{\kappa}\exp(\mathrm{i}\kappa_1 x_1 + \mathrm{i}\kappa_2 x_2) + \frac{\mathbf{E}_{\mathrm{I}}^{-}\mathbf{P} - \overline{\mathbf{E}}_{\mathrm{I}}^{+}\overline{\mathbf{Q}}}{\kappa}\exp(-\mathrm{i}\kappa_1 x_1 - \mathrm{i}\kappa_2 x_2), \tag{30}$$

$$\mathbf{t}_{\mathrm{I}} = \left(\overline{\mathbf{T}}_{\mathrm{I}}^{-}\overline{\mathbf{P}} + \mathbf{T}_{\mathrm{I}}^{+}\mathbf{Q}\right)\exp(\mathrm{i}\kappa_1 x_1 + \mathrm{i}\kappa_2 x_2) + \left(\mathbf{T}_{\mathrm{I}}^{-}\mathbf{P} + \overline{\mathbf{T}}_{\mathrm{I}}^{+}\overline{\mathbf{Q}}\right)\exp(-\mathrm{i}\kappa_1 x_1 - \mathrm{i}\kappa_2 x_2), \tag{31}$$

where matrices $\mathbf{T}_{\mathrm{I}}^{\pm}$ and $\mathbf{E}_{\mathrm{I}}^{\pm}$ are

$$\begin{aligned}
T^{-}_{\mathrm{I}lj} &= \sum_{a=1}^{3} L_{\mathrm{I}la}L^{-1}_{\mathrm{I}aj}\exp(-\mathrm{i}\kappa p_{\mathrm{I}a}x_3),\\
T^{+}_{\mathrm{I}lj} &= \sum_{a=1}^{3} L_{\mathrm{I}la}L^{-1}_{\mathrm{I}aj}\exp(\mathrm{i}\kappa p_{\mathrm{I}a}x_3),\\
E^{-}_{\mathrm{I}lj} &= \mathrm{i}\sum_{a=1}^{3} A_{\mathrm{I}la}L^{-1}_{\mathrm{I}aj}\exp(-\mathrm{i}\kappa p_{\mathrm{I}a}x_3),\\
E^{+}_{\mathrm{I}lj} &= \mathrm{i}\sum_{a=1}^{3} A_{\mathrm{I}la}L^{-1}_{\mathrm{I}aj}\exp(\mathrm{i}\kappa p_{\mathrm{I}a}x_3).
\end{aligned} \tag{32}$$

Matrices $\mathbf{T}_{\mathrm{I}}^{\pm}$ are dimensionless, and matrices $\mathbf{E}_{\mathrm{I}}^{\pm}$ have the dimension of the compliance tensor. Matrices $\mathbf{E}_{\mathrm{I}}^{\pm}$ relate to matrices $\mathbf{T}_{\mathrm{I}}^{\pm}$ as $\mathbf{E}_{\mathrm{I}}^{\pm} = \mathbf{B}_{\mathrm{I}}\mathbf{T}_{\mathrm{I}}^{\pm}$. One can obtain $\mathbf{T}_{\mathrm{I}}^{-}$ from $\mathbf{T}_{\mathrm{I}}^{+}$, $\mathbf{E}_{\mathrm{I}}^{-}$ from $\mathbf{E}_{\mathrm{I}}^{+}$, by replacing variable x_3 to $-x_3$, and vice versa. See Appendix A for the explicit expressions of those matrices when the material is isotropic.

One can easily confirm from (32) that $\mathbf{T}_{\mathrm{I}}^{\pm}|_{x_3=0} = \mathbf{I}$, and $\mathbf{E}_{\mathrm{I}}^{\pm}|_{x_3=0} = \mathbf{B}_{\mathrm{I}}$. ($\mathbf{I}$ is the identity matrix.) For one real-valued Fourier component (18) of the traction vector on the substrate surface, the above consideration and Eq. (31) leads to

$$\mathbf{P} + \overline{\mathbf{Q}} = \bar{\mathbf{a}}. \tag{33}$$

At the layer interface $x_3 = -d$, the continuity conditions give rise to $\mathbf{u}_{\mathrm{I}} = \mathbf{u}_{\mathrm{II}}$ and $\mathbf{t}_{\mathrm{I}} = \mathbf{t}_{\mathrm{II}}$. (The uniform residual stresses in the substrate layers have only trivial Fourier components for any nontrivial wavenumber, and therefore won't affect the above continuity conditions.) Layer II itself is semi-infinite, so that by Section 4, $\mathbf{u}_{\mathrm{II}}$ and $\mathbf{t}_{\mathrm{II}}$ at the interface must satisfy the same relation as that between (18) and (21). The above considerations lead to

$$\mathbf{E}_{\mathrm{I}}^{-}\mathbf{P} - \overline{\mathbf{E}}_{\mathrm{I}}^{+}\overline{\mathbf{Q}} = \mathbf{B}_{\mathrm{II}}\left(\mathbf{T}_{\mathrm{I}}^{-}\mathbf{P} + \overline{\mathbf{T}}_{\mathrm{I}}^{+}\overline{\mathbf{Q}}\right), \tag{34}$$

where matrices $\mathbf{T}_{\mathrm{I}}^{\pm}$ and $\mathbf{E}_{\mathrm{I}}^{\pm}$ are all evaluated at $x_3 = -d$.

Define two bimaterial matrices:

$$\mathbf{H}_1 = \mathbf{B}_{\mathrm{I}} - \mathbf{B}_{\mathrm{II}}, \tag{35}$$

$$\mathbf{H}_2 = \overline{\mathbf{B}}_{\mathrm{I}} + \mathbf{B}_{\mathrm{II}}. \tag{36}$$

The latter is a positive-definite Hermitian.

From Eqs. (33)–(36), vectors $\mathbf{P}$ and $\mathbf{Q}$ can be determined by solving

$$\begin{bmatrix} \mathbf{X} & -\mathbf{Y} \\ \mathbf{I} & \mathbf{I} \end{bmatrix} \begin{pmatrix} \mathbf{P} \\ \overline{\mathbf{Q}} \end{pmatrix} = \begin{pmatrix} \mathbf{0} \\ \bar{\mathbf{a}} \end{pmatrix}, \tag{37}$$

where $\mathbf{X} = \mathbf{H}_1 \mathbf{T}_{\mathrm{I}}^{-}|_{x_3=-d}$ and $\mathbf{Y} = \mathbf{H}_2 \overline{\mathbf{T}}_{\mathrm{I}}^{+}|_{x_3=-d}$.

Consequently, for one real-valued Fourier component, the elastic energy stored in the substrate per period is given by

$$\frac{\kappa_1 \kappa_2}{(2\pi)^2} \int_{-\pi/\kappa_2}^{\pi/\kappa_2} \int_{-\pi/\kappa_1}^{\pi/\kappa_1} \frac{1}{2} \mathbf{t}^{\mathrm{T}} \cdot \mathbf{u} \, \mathrm{d}x_1 \, \mathrm{d}x_2 = \frac{\mathbf{a}^{\mathrm{T}} \mathbf{F} \bar{\mathbf{a}}}{\kappa}, \tag{38}$$

where $\mathbf{F} = \mathrm{Re}\left\{ \mathbf{B}_{\mathrm{I}} (\mathbf{X} + \mathbf{Y})^{-1} \mathbf{Y} - \overline{\mathbf{B}}_{\mathrm{I}} (\mathbf{X} + \mathbf{Y})^{-1} \mathbf{X} \right\}$. Re stands for the real part of a complex number. Not only does the matrix $\mathbf{F}$ depend on (h_1, h_2) and the stiffness tensors of the two layers, also it is a function of κd. Denote $\mathbf{F} = \mathbf{F}(c_{\mathrm{I}ijkl}, c_{\mathrm{II}ijkl}, \theta, \kappa d)$.

When layer I and II are of the same material and crystalline orientation, $\mathbf{H}_1 = \mathbf{0}$, so that $\mathbf{P} = \bar{\mathbf{a}}$, $\mathbf{Q} = \mathbf{0}$, and $\mathbf{F} = \mathbf{M}$, recovering the results in Eqs. (18), (21), and (22). When layer II is a rigid material, $\mathbf{B}_{\mathrm{II}} = \mathbf{0}$, so that $\mathbf{X} = \mathbf{E}_{\mathrm{I}}^{-}|_{x_3=-d}$ and $\mathbf{Y} = \overline{\mathbf{E}}_{\mathrm{I}}^{+}|_{x_3=-d}$. When layer II is absent or extremely compliant, Eq. (34) becomes $\mathbf{T}_{\mathrm{I}}^{-} \mathbf{P} + \overline{\mathbf{T}}_{\mathrm{I}}^{+} \overline{\mathbf{Q}} = \mathbf{0}$ at $x_3 = -d$, so we can let $\mathbf{X} = -\mathbf{T}_{\mathrm{I}}^{-}|_{x_3=-d}$ and $\mathbf{Y} = \overline{\mathbf{T}}_{\mathrm{I}}^{+}|_{x_3=-d}$.

When the concentration field is represented as Eq. (8), from (9), (10), (18), (19), and (38), the elastic free energy per unit area can be written as

$$\widetilde{G}_{\mathrm{elastic}} = -\phi^2 \left(\frac{2\pi}{\lambda} \right) \sum_{n=1}^{+\infty} \left(n C_n^2 \Theta_n \right), \tag{39}$$

where

$$\Theta_n = \mathbf{m}^{\mathrm{T}} \mathbf{F} \left(c_{\mathrm{I}ijkl}, c_{\mathrm{II}ijkl}, \theta, \frac{2n\pi d}{\lambda} \right) \mathbf{m}, \tag{40}$$

and vector $\mathbf{m}$ has been given by Eq. (25). Only the terms Θ_n in Eq. (39) depend on θ, but they are also functions of n. To minimize Eq. (39) with respect to θ, one needs to know all the Fourier components C_n of the concentration field, which in turn depend on Θ_n and the detailed forms of g_{m} and g_{b} in Eq. (7). Nonetheless, one single Fourier mode of the concentration field already gives a good approximation (Gao et al., 2002). Consequently, to determine the equilibrium orientation of a set of periodic stripes on a layered substrate, we minimize $-\Theta_1$ as a function of θ with varying surface stress anisotropy R, stiffness tensors of the two layers, and d/λ (the normalized thickness of the first layer). In the next three subsections, we concentrate on stiffness anisotropy, so that the surface stress tensor is assumed isotropic and fixed.

5.1. A layered substrate of two isotropic materials

Recall the inspection that the elastic free energy is linear in the compliance tensor since the traction boundary condition is prescribed. If one uses a thin elastic substrate, the added compliance amplifies the effect of elasticity, reducing the equilibrium phase size. One can even tune the equilibrium phase size by the following hypothetical experiment. At a certain time, periodic stripes of period λ are at equilibrium on a

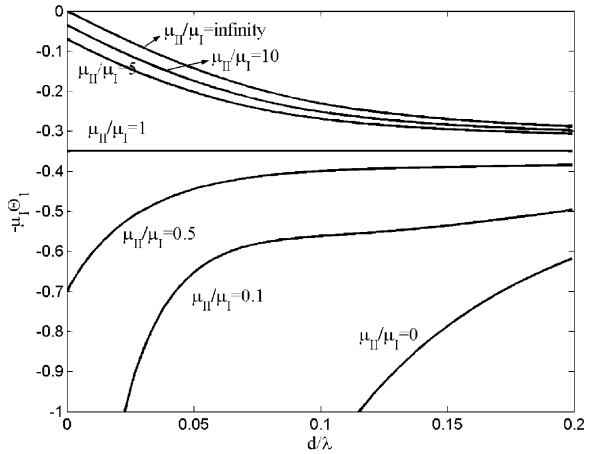

Fig. 5. $-\mu_I\Theta_1$ as a function of d/λ with varying shear modulus ratio μ_{II}/μ_I of the two dissimilar isotropic materials in the substrate.

homogeneous semi-infinite (or thick) substrate. Cut the substrate at $x_3 = -d$, and bond the thin layer–monolayer system with another material that becomes layer II in Fig. 1. On annealing, atoms in the monolayer will relocate on the substrate surface, and stripes will reach a new equilibrium period λ'. The ratio of the elastic constants and the thickness of the first layer can be varied, giving rise to a tunable λ'.

In this section, the two substrate layers are assumed to be elastically isotropic, so that the stripe orientation is of no concern here. The elastic free energy is approximately measured by $-\mu_I\Theta_1$. Consequently, if this quantity decreases, we will obtain a stronger elastic interaction and, accordingly, a smaller equilibrium phase size, i.e., $\lambda' < \lambda$. Let Poisson's ratios equal, $\nu_I = \nu_{II} = 0.3$. Fig. 5 plots $-\mu_I\Theta_1$ as a function of d/λ with varying shear modulus ratio μ_{II}/μ_I. We next discuss the results.

When the substrate is of a single isotropic material ($\mu_{II}/\mu_I = 1$), obviously, $-\mu_I\Theta_1$ does not change with respect to d/λ. This is our reference state. When d/λ is fixed, if layer II is more compliant ($\mu_{II}/\mu_I < 1$), $-\mu_I\Theta_1$ becomes smaller; if layer II is stiffer ($\mu_{II}/\mu_I > 1$), $-\mu_I\Theta_1$ becomes larger. When μ_{II}/μ_I is fixed, with decreasing d/λ, the function $-\mu_I\Theta_1$ increases if $\mu_{II}/\mu_I > 1$, or decreases if $\mu_{II}/\mu_I < 1$. Consequently, to amplify the equilibrium phase size ($\lambda' > \lambda$), one can use a compliant material for layer II; to shrink the size ($\lambda' < \lambda$), a stiff material for layer II. In both cases, the purpose is more easily satisfied by making the first layer as thin as possible. Also Fig. 5 shows that an extremely compliant material or nothing for layer II ($\mu_{II}/\mu_I = 0$) can remarkably change the elastic interaction, and the effect is unprecedented for a layered substrate even with a very small shear modulus ratio, e.g., $\mu_{II}/\mu_I = 0.1$.

5.2. A layered substrate of an isotropic material on a cubic crystal

Certain kinds of atoms can only form patterns on surfaces of some specific materials, which may not provide the desired orientation preference. Without sacrificing the properties determined by the monolayer and layer I, we can choose a layer II with the required stiffness anisotropy. This section shows that the stiffness anisotropy of layer II can be passed to the monolayer patterns through the elastic field.

As an example, consider a layered substrate of an isotropic material on the Cu(1 0 0) surface. Let the x_1 axis be in the direction $\langle 0\,1\,0\rangle$, and x_2 in $\langle 0\,0\,1\rangle$. Assume that the c_{11} component of the stiffness tensor of the isotropic material is equal to that of the copper. Fig. 6 plots $-c_{11}\Theta_1$ as a function of θ with different thicknesses of the isotropic layer. When $d/\lambda = 0$, $-c_{11}\Theta_1$ minimizes at $\theta_{eq} = 0°$ and $\theta_{eq} = 90°$, retaining the orientation preference of the Cu(1 0 0) surface (as predicted by Section 4.1). When d/λ is sufficiently large, $-c_{11}\Theta_1$ becomes a constant, because there is no orientation preference for the isotropic layer.

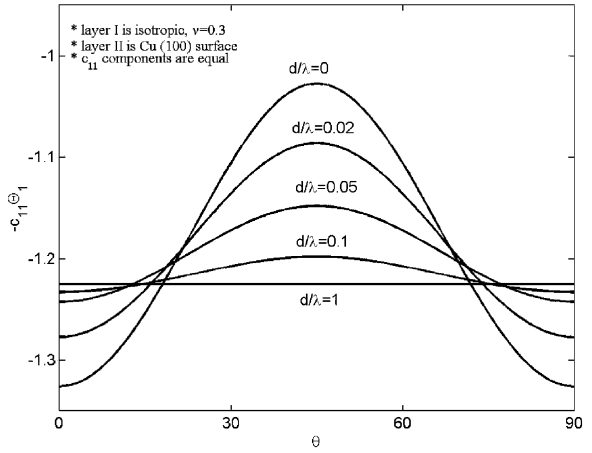

Fig. 6. $-c_{11}\Theta_1$ as a function of θ with varying d/λ. The substrate consists of an isotropic material (layer I) and a cubic crystal (layer II).

5.3. A layered substrate of two cubic crystals

In general, the stripe orientation depends on the thicknesses and the degrees of the stiffness anisotropy of the substrate layers. Let us consider a set of stripes on the Cu(1 0 0) surface. Cut the substrate at plane $x_3 = -d$, rotate the thin layer–monolayer system about the x_3 axis by 45°, and bond it with the remaining bulk copper. This *fictitious* substrate is used to illustrate the competition between two layers of different orientation preferences. On annealing, stripes may or may not rotate by 45°. Let the coordinates x_i coincide with the crystalline axes of layer II. A tensor transformation gives the stiffness components in layer I. Obviously, when layer I is very thick, the stripe orientation follows the preference of layer I, i.e., $\theta_{eq} = 45°$. When layer I is very thin, the orientation follows the preference of layer II, i.e., $\theta_{eq} = 0°$ and $\theta_{eq} = 90°$.

Fig. 7(a) plots $-c_{11}\Theta_1$ as a function of θ with varying d/λ, illustrating several kinds of behaviors. When $d/\lambda < 0.03858$, $-c_{11}\Theta_1$ minimizes at $\theta_{eq} = 0°$ and 90°. When $0.03858 < d/\lambda < 0.0399$, $-c_{11}\Theta_1$ minimizes at certain angles off the axes. When $d/\lambda > 0.0399$, $-c_{11}\Theta_1$ minimizes at $\theta_{eq} = 45°$. Fig. 7(b) plots the

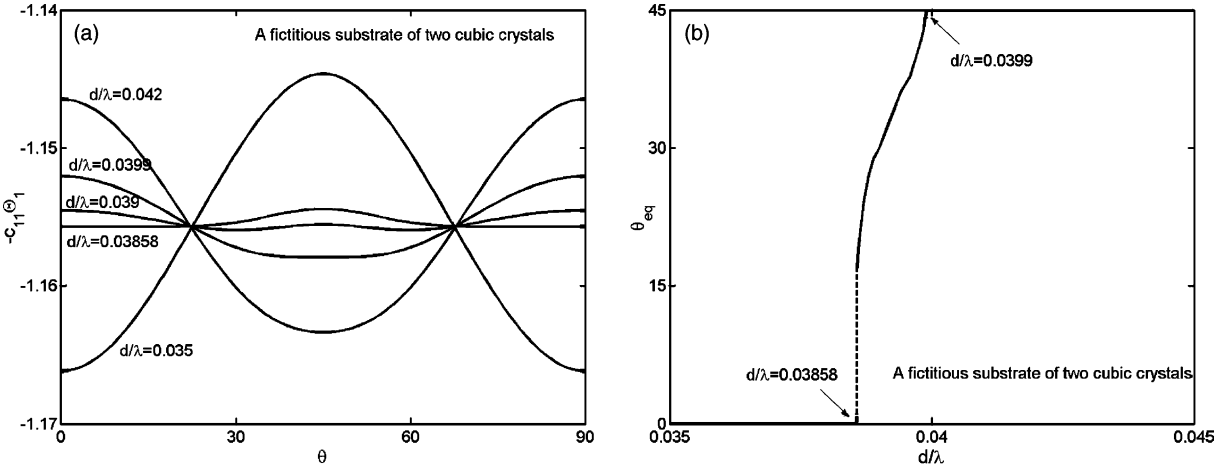

Fig. 7. (a) $-c_{11}\Theta_1$ as a function of θ with varying d/λ. (b) The equilibrium orientation θ_{eq} as a function of d/λ. The substrate is fictitious (see text).

equilibrium orientation θ_{eq} as a function of d/λ. Due to symmetry, we restrict $0^\circ \leqslant \theta_{eq} \leqslant 45^\circ$. The transitions between the along-axis stripes and off-axis stripes can be of the first- or second-order.

6. Discussion

Self-organization on solid surfaces has been recognized as a promising way of growing uniform nanostructures with long-range orders and regular sizes. The self-assembled phase patterns can be manipulated by engineering the long-range elastic field. The system is analogous with an oscillator. A static force applied to the oscillator does not change its vibrating frequency. Similarly, applying a uniform stress field in the plane of the layer, e.g., through bending, does not affect the patterns. Nonetheless, one can use a substrate with various crystalline symmetries. The orientation of a set of periodic stripes only depends on the anisotropy in the surface stress and the substrate stiffness tensor. Furthermore, this paper shows the possibilities of a layered substrate. In this case, the orientation dependence involves the concentration field within the stripes, but can be determined approximately by using the leading Fourier mode of the concentration field. The equilibrium phase size and orientation are tunable with various material and structural selections of the substrate layers. The elastic field in the anisotropic, heterogeneous, three-dimensional half-space is solved by extending the Eshelby–Stroh–Lekhnitskii formalism. The Fourier representation simplifies the solution and enables our parametric study.

Our calculations (Sections 5.2 and 5.3) show that in order for the stiffness anisotropy of layer II to be in effect pronouncedly, the thickness of the first layer d/λ must be very thin compared with the feature size of those patterns. Experiments tell us that typically $\phi \sim 4$ N/m, $c_{11} \sim 10^{11}$ N/m^2, and λ ranges from nanometers to micrometers. Take $\lambda \sim 10$ nm, $|c_{11}\Theta_1| \sim 1$, and $C_1 = 0.4$, and we can obtain that the elastic free energy per unit area (39) is about 1 J /m^2, which is on the same order of 1 eV free energy per atomic site on a solid surface (Somorjai, 1994). In order for the orientation preference to be effective, the variation of function $-c_{11}\Theta_1$ with respect to angle θ should be also comparable with this magnitude. From Fig. 6, we can conclude that d/λ must be smaller than 0.1, which says that if λ is 100 nm, the thickness of the thin layer should be about 10 nm.

Though our cut-and-bond method may not be realistic to make a substrate with ultrathin layers, there are many other ways, e.g., through epitaxial growth etc. One can tune the strain and stress inside the layers by the lattice misfit between the different layers. The patterns, however, won't be affected if the interfaces between layers are flat. (The reason has been stated in the first paragraph of this section.) By contrast, we can use the scheme proposed by Fig. 8(b). It is well known that during thin film growth, morphological patterns can form upon strain relaxation. One can grow an additional layer of material on such a rough surface. Monolayer patterns will unavoidably be affected by the buried topographic pattern because (i) the compliance tensor of the substrate composite is spatially nonuniform in plane (x_1, x_2); (ii) the residual stress in the first layer (probably due to lattice misfit or thermal expansion mismatch) is nonuniform. Consequently, one can make patterns with spatially varying feature size and orientation. This scheme of using an external pattern is an example of guided self-assembly (Gao and Suo, 2003a). One variation of this scheme is shown in Fig. 8(c). A void or inclusion buried underground serves the same purpose.

A recent experiment points out another possibility. Ellmer et al. (2001) studied nitrogen on the Cu(1 0 0) surface. After annealing, the surface was covered by a regular square lattice of nitrogen islands, approximately 5 nm across, with the sides parallel to the [0 0 1] direction (consistent with our predictions in Section 4.1). A small amount of gold, pre-deposited on the bare copper surface, changed the elastic properties of the substrate by forming a marginal region of Au–Cu alloy, as schematically shown in Fig. 8(a). On this Au-doped surface, nitrogen atoms again formed square lattices, but with the sides parallel to [0 1 1] direction. So far we don't know quantitatively how the elastic constants change due to Au-doping. Our calculations in

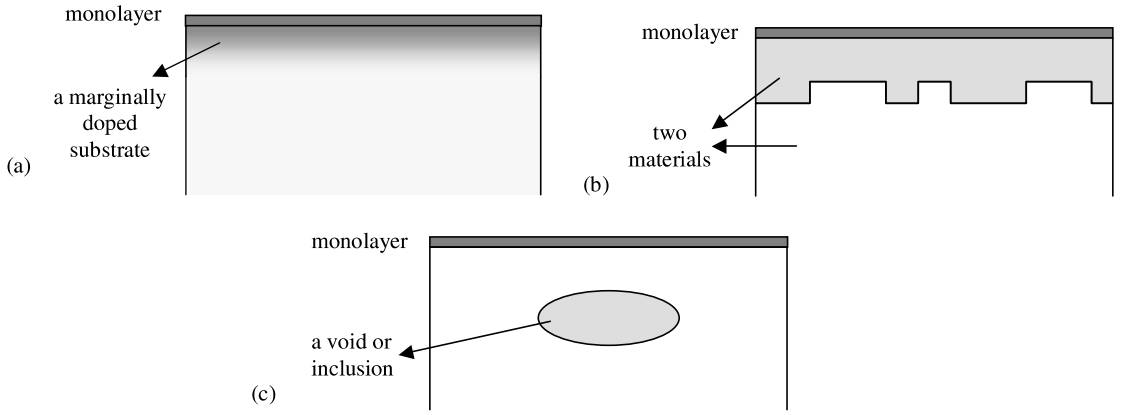

Fig. 8. Manipulating the monolayer phase patterns by using a substrate: (a) with a marginally doped region; (b) with a buried topographic pattern; (c) with a buried void or inclusion.

Section 5 suggest that this new region should prefer different orientations from the Cu(1 0 0) surface. We are awaiting further experimental development along this line to test our argument.

Acknowledgements

Discussions with Z. Suo and H.H. Yu were very helpful. This work was partially supported by the Department of Energy through contract DE-FG02-99ER45787.

Appendix A

One can transform a given elastic stiffness tensor in the coordinates (x_1, x_2, x_3) to (x, y, x_3). The stiffness components that are related to the plane elastic field in (x, x_3) can be used to analytically compute the eigenvalues p_a and matrices **A**, **L**, and **B** (Eshelby et al., 1953; Stroh, 1958; Lekhnitskii, 1963; Ting, 1996). Nonetheless, numerical calculation is much more convenient, especially when dealing with the layered structures.

The Eshelby–Stroh–Lekhnitskii representation may break down if the eigenvalue problem is degenerate. For example, when the material is elastically isotropic, the eigenvalue problem (12) has repeated eigenvalues $p_1 = p_2 = p_3 = \mathrm{i}$, and matrices **A**, **L** are singular. The Stroh matrix $\mathbf{B} = \mathrm{i}\mathbf{A}\mathbf{L}^{-1}$, however, has smooth limit, which is determined as follows. We can introduce a small degree of anisotropy in the stiffness tensor, and compute the Stroh matrix. By reducing this degree of anisotropy to zero, we can obtain the analytical form for the Stroh matrix, and similarly for matrices $\mathbf{T}^{\pm}$ and $\mathbf{E}^{\pm}$.

Of particular importance is the following set of results for an isotropic material:

$$\mathbf{B} = \frac{1}{\mu}\begin{bmatrix} 1-v & 0 & \mathrm{i}\left(\frac{1}{2}-v\right) \\ 0 & 1 & 0 \\ -\mathrm{i}\left(\frac{1}{2}-v\right) & 0 & 1-v \end{bmatrix}, \tag{A.1}$$

$$\mathbf{T}^{-} = \begin{bmatrix} 1+s & 0 & \mathrm{i}s \\ 0 & 1 & 0 \\ \mathrm{i}s & 0 & 1-s \end{bmatrix} \exp(s), \tag{A.2}$$

$$\mathbf{T}^{+}=\begin{bmatrix}1-s & 0 & -\mathrm{i}s\\ 0 & 1 & 0\\ -\mathrm{i}s & 0 & 1+s\end{bmatrix}\exp(-s), \tag{A.3}$$

$$\mathbf{E}^{-}=\frac{1}{\mu}\begin{bmatrix}1-v+\frac{s}{2} & 0 & \frac{\mathrm{i}}{2}(1-2v+s)\\ 0 & 1 & 0\\ -\frac{\mathrm{i}}{2}(1-2v-s) & 0 & 1-v-\frac{s}{2}\end{bmatrix}\exp(s), \tag{A.4}$$

$$\mathbf{E}^{+}=\frac{1}{\mu}\begin{bmatrix}1-v-\frac{s}{2} & 0 & \frac{\mathrm{i}}{2}(1-2v-s)\\ 0 & 1 & 0\\ -\frac{\mathrm{i}}{2}(1-2v+s) & 0 & 1-v+\frac{s}{2}\end{bmatrix}\exp(-s), \tag{A.5}$$

where $s=\kappa d$, and μ and v are the shear modulus and Poisson's ratio respectively. These results are given in the coordinates (x,y,x_3).

References

Alerhand, O.L., Vanderbilt, D., Meade, R.D., Joannopoulos, J.D., 1988. Spontaneous formation of stress domains on crystal surfaces. Phys. Rev. Lett. 61, 1973–1976.

Ellmer, H., Repain, V., Rousset, S., Croset, B., Sotto, M., Zeppenfeld, P., 2001. Self-ordering in two dimensions: nitrogen adsorption on copper (1 0 0) followed by STM at elevated temperature. Surf. Sci. 476, 95–106.

Eshelby, J.D., Read, W.T., Shockley, W., 1953. Anisotropic elasticity with applications to dislocation theory. Acta Metall. 1, 251–259.

Gao, Y.F., Lu, W., Suo, Z., 2002. A mesophase transition in a binary monolayer on a solid surface. Acta Mater. 50, 2297–2308.

Gao, Y.F., Suo, Z., 2003a. Guided self-assembly of molecular dipoles on a substrate surface. J. Appl. Phys. 93, 4276–4282.

Gao, Y.F., Suo, Z., 2003b. The orientation of the self-assembled monolayer stripes on a crystalline substrate. J. Mech. Phys. Solids 51, 147–167.

Gurtin, M.E., Murdoch, A.I., 1976. Effect of surface stress on wave propagation in solids. J. Appl. Phys. 47, 4414–4421.

Ibach, H., 1997. The role of surface stress in reconstruction, epitaxial growth and stabilization of mesoscopic structures. Surf. Sci. Rep. 29, 195–263, Erratum;
Surf. Sci. Rep. 35, 71–73.

Kern, K., Niehus, H., Schatz, A., Zeppenfeld, P., Goerge, J., Comsa, G., 1991. Long-range spatial self-organization in the adsorbate-induced restructuring of surfaces: Cu{1 1 0}-(2×1)O. Phys. Rev. Lett. 67, 855–858.

Lekhnitskii, S.G., 1963. Theory of Elasticity of an Anisotropic Body. Holden-Day, San Francisco.

Lu, W., Suo, Z., 2002a. Symmetry breaking in self-assembled monolayers on solid surface. I. Anisotropic surface stress. Phys. Rev. B. 65, 085401.

Lu, W., Suo, Z., 2002b. Symmetry breaking in self-assembled monolayers on solid surfaces. II. Anisotropic substrate elasticity. Phys. Rev. B. 65, 205418.

Murdoch, A.I., 1976. The propagation of surface waves in bodies with material boundaries. J. Mech. Phys. Solids 24, 137–146.

Ng, K.-O., Vanderbilt, D., 1995. Stability of periodic domain structures in a two-dimensional dipolar model. Phys. Rev. B 52, 2177–2183.

Pohl, K., Bartelt, M.C., de la Figuera, J., Bartelt, N.C., Hrbek, J., Hwang, R.Q., 1999. Identifying the forces responsible for self-organization of nanostructures at crystal surfaces. Nature 397, 238–241.

Somorjai, G.A., 1994. Introduction to Surface Chemistry and Catalysis. Wiley-Interscience, New York.

Stroh, A.N., 1958. Dislocations and cracks in anisotropic elasticity. Philos. Mag. 7, 625–646.

Suo, Z., 1990. Singularities, interfaces and cracks in dissimilar anisotropic media. Proc. R. Soc. Lond. A 427, 331–358.

Suo, Z., Lu, W., 2000. Composition modulation and nanophase separation in binary epilayer. J. Mech. Phys. Solids 48, 211–232.

Ting, T.C.T., 1996. Anisotropic Elasticity: Theory and Applications. Oxford University Press, UK.

Thomson, R., Chuang, T.-J., Lin, I.-H., 1986. The role of surface stress in fracture. Acta Metall. 34, 1133–1143.

Zeppenfeld, P., Krzyzowski, M.A., Romainczyk, Ch., David, R., Comsa, G., Röder, H., Bromann, K., Brune, H., Kern, K., 1995. Stability of disk and stripe patterns of nanostructures at surfaces. Surf. Sci. 342, L1131–L1136.